

Thermally Activated Transformations of 2D Nonautonomous Phases and Contraction of Polycrystalline Oxide Materials

V. V. Gusarov, A. A. Malkov, A. A. Malygin, and S. A. Suvorov

St. Petersburg State Technical University, ul. Politekhnikeskaya 29, St. Petersburg, 195251 Russia

Received March 21, 1994

INTRODUCTION

As follows from experiments, sintering of polycrystalline materials, creep, solid-state synthesis, and related processes are activated, in most cases, when a certain temperature, the so-called Tammann temperature [1 - 4] is attained. Theoretical models based on continuous Arrhenius-type temperature dependences of diffusion coefficients cannot describe the abrupt increase in the rates of the above processes as a function of increasing temperature. As we have shown earlier [5 - 7], the temperatures of the abrupt increase in the rates of solid-state processes correlate with the melting temperatures of 2D nonautonomous phases. To clarify the term "nonautonomous phase," note that it was introduced by R. Defay in 1934 and was widely used for analyzing surface states in the monograph [8]. The concept of the nonautonomous phase can be used in describing a variety of systems; examples are the dislocations and the regions where regular phases are in contact with one another [9]. We classify nonautonomous phases as one-, two-, and three-dimensional according to the number of linearly independent non-collinear directions that allow the invariant translation of the system. The effectiveness of this concept was demonstrated in [7, 10 - 14].

RESULTS AND DISCUSSION

In polycrystalline materials, 2D nonautonomous phases include intergranular and interphase boundary regions, as well as regions adjacent to free surfaces. Melting points of 2D nonautonomous phases can be calculated, to a first approximation, by the equation [6]

$$T_{m(2-n)} = \frac{1 - \alpha_H}{1 - \alpha_S} T_m, \quad (1)$$

where α_H and α_S are parameters depending on enthalpy and entropy of the substance [6], and T_m is the melting temperature (K) of the autonomous phase of the same composition. For a large number of compounds, $(1 - \alpha_H)/(1 - \alpha_S) = 0.65 \pm 0.05$ [6]; that is, $T_{m(2-n)}$ is approximately equal to the Tammann temperature ($T_T \approx 2T_m/3$) [1]. Given that the melting points of 2D nonautonomous phases coincide with activation tem-

peratures of solid-state processes, it can be inferred that, in polycrystalline materials, the melting of 2D nonautonomous phases is a key transformation: to control this transformation is to control, to a great extent, the evolution of a polycrystalline system.

According to equation (1), the major parameter determining the $T_{m(2-n)}$ value is the chemical composition of the 2D nonautonomous phase. Chemical composition of this phase can be changed by adding small amounts of an impurity that segregate at grain boundaries. A particular way of introducing the impurity can be chosen based on the difference $\Delta\sigma$ between surface energies of the major phase and the impurity phase, and also on transformational and transport properties of the nonautonomous phase. Among these properties are the rate of autonomous-to-nonautonomous phase transformation and rheological constants, in particular, viscosity of the liquid nonautonomous phase. Indeed, the rates of attaining local equilibrium within the regions adjacent to the surface of the major component are found to be highly consistent with $\Delta\sigma$ values of the components, the $MO_n-FeO_{1.5}$ systems (where M = Be, Al, Si) being an example. Starting materials used in studies of these systems are specified in Table 1. The relaxation kinetics (Figs. 1, 2) was studied using Mössbauer spectroscopy according to the technique described in [15].

As follows from the kinetic curves (Fig. 1), relaxation rates increase drastically in the range 1270 - 1370 K, which overlaps with the interval $T_{m(2-n)} = 1200 \pm 100$ K calculated for the 2D nonautonomous phase consisting of Fe(III) oxide. As is seen in Fig. 2, the BeO- $FeO_{1.5}$ system, characterized by a great difference in the surface energies of the major and the impurity components, exhibits a high rate of local equilibration in grain-boundary regions. This fact leads to the conclusion that, in such systems, the rates of solid-state processes are affected relatively little by impurity introduction, which is also confirmed by the observations reported in [11 - 17]. Conversely, when the surface energy of the impurity phase differs only slightly from that of the major substance (as in the $AlO_{1.5}-FeO_{1.5}$, $AlO_{1.5}-SiO_2$, $AlO_{1.5}-TiO_2$, and $SiO_2-FeO_{1.5}$ systems, see Table 2) and, accordingly, relaxation rates are low (Fig. 2), the tightness of the contact of components

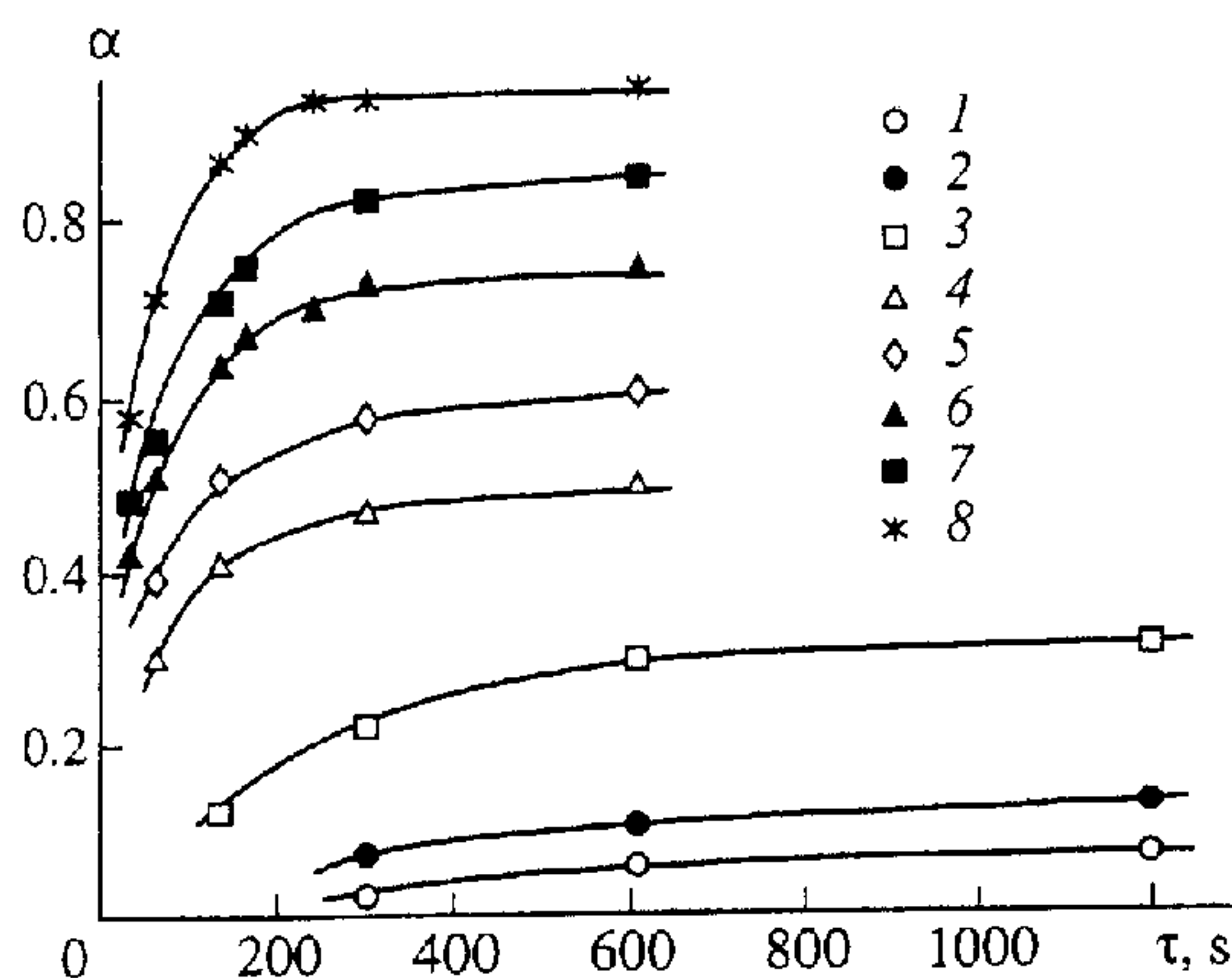


Fig. 1. The fraction of Fe(III) oxide transferred to the 2D nonautonomous phase as a function of the time of isothermal annealing at 1070, 1170, 1270, 1370, 1420, 1470, 1520, and 1570 K (curves 1 - 8, respectively). The initial state of the samples is characterized in Table 1.

in the starting materials (which is determined by the manner in which impurity was introduced) should play a decisive role.

Consider the latter case, taking alumina sintering as an example. The surface energy of the α - $\text{AlO}_{1.5}$ phase is relatively low, as compared with that of materials known as active sintering aids for alumina. In some cases, the alumina surface energy is even lower than that of an additive (Table 2). Therefore, the rate of the surface relaxation in alumina grains depends substantially on the technique for introducing the additive. The best conjugation of the components is provided by the molecular layering technique, which does not affect the phase composition and structural state of the major component [20, 21]. The opposite situation (concerning the conjugation degree) occurs if mechanical mixing is used for introducing additives.

We studied the sintering of alumina (GK grade according to the Soviet State Standard GOST 6912-87) with small amounts of TiO_2 additive (Table 3) introduced by the two above-mentioned techniques. We measured the contraction of the samples during heating from 300 to 1850 K at a constant rate of 3 K/min, with an Opton Model 1600 D dilatometer. The starting samples dif-

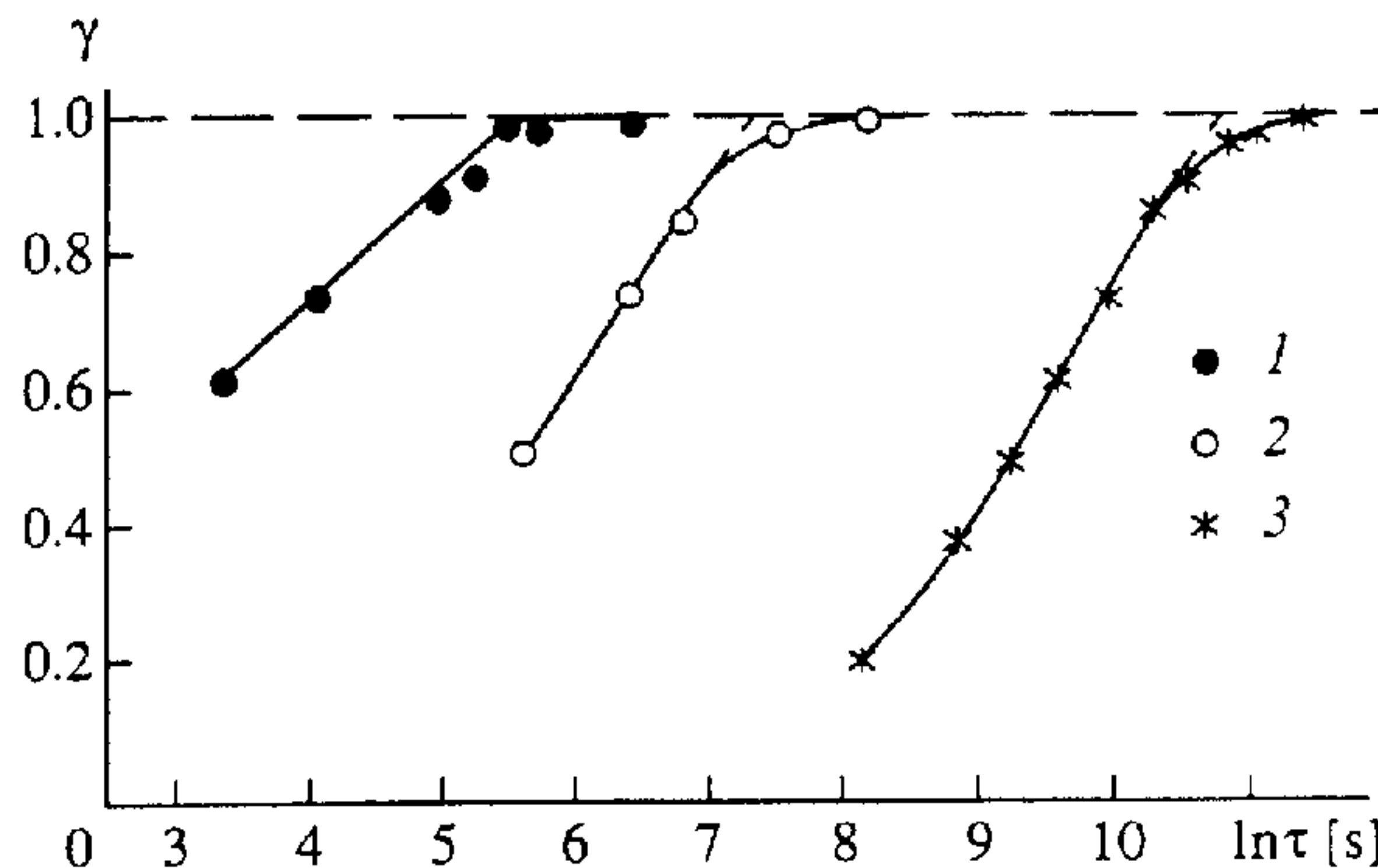


Fig. 2. Time dependences of the fraction of Fe(III) oxide transferred to the 2D nonautonomous phase at 1570 K for the (1) $\text{BeO}-\text{FeO}_{1.5}$, (2) $\text{AlO}_{1.5}-\text{FeO}_{1.5}$, and (3) $\text{SiO}_2-\text{FeO}_{1.5}$ systems. The initial state of the samples is characterized in Table 1, $\gamma = \alpha/\alpha_{\text{max}}$, where α is the mole fraction of Fe_2O_3 concentrated in the 2D nonautonomous phase.

ferred in density by no more than 2% (Table 3). The obtained data are displayed in Fig. 3.

Contraction of the samples prepared by molecular layering began at a definite temperature equal to the melting temperature of the 2D nonautonomous phase consisting of TiO_2 , $T_{m(2-n)} = 1380 \pm 100$ K. For the samples prepared by molecular mixing, the onset of the contraction was less distinct; the whole process was extended in time and temperature and was shifted to higher temperatures by 50 - 100 K. The reason for the disparity is as follows. When molecular layering was used for modifying alumina with TiO_2 , the autonomous phase of the powder material was covered, starting at 1380 K, with a layer of a nonautonomous TiO_2 -rich liquid phase. On the contrary, in samples prepared by mechanical mixing, the TiO_2 -rich nonautonomous liquid phase, which was formed at the contact of alumina and TiO_2 grains, expanded over the surface of alumina particles at a rather slow rate, because of the relatively low $\Delta\sigma$ value inherent in the $\text{AlO}_{1.5}-\text{TiO}_2$ system (see Table 2).

Note that the transition of the autonomous Fe_2O_3 phase to the 2D nonautonomous phase, activated by the presence of Be, Al, and Si oxides, is characterized by relaxation times of 2.5×10^2 , 1.5×10^3 , and 4.5×10^4 s, respectively (Fig. 2). Comparing surface energies of the

Table 1. Properties of the mixtures heat-treated between 1070 and 1570 K (particle size, less than 63 μm ; component added - hematite)

Mixture	Fe_2O_3 , mole fraction	Main component: structure and purity	S_{sp} , m^2/g
$\text{BeO} + \text{FeO}_{1.5}$	0.01	Bromellite; reagent-grade Be nitrate; TU 6-09-2358-77	11 ± 2
$\text{AlO}_{1.5} + \text{FeO}_{1.5}$	0.01	Corundum; Al_2O_3 (reagent grade, spectrograde; TU 6-09-2358-77)	6.5 ± 0.4
$\text{SiO}_2 + \text{FeO}_{1.5}$	0.006	Amorphous; Aerosil A300 GOST 14922-77	300 ± 20

Note: S_{sp} is the specific surface of the major component.

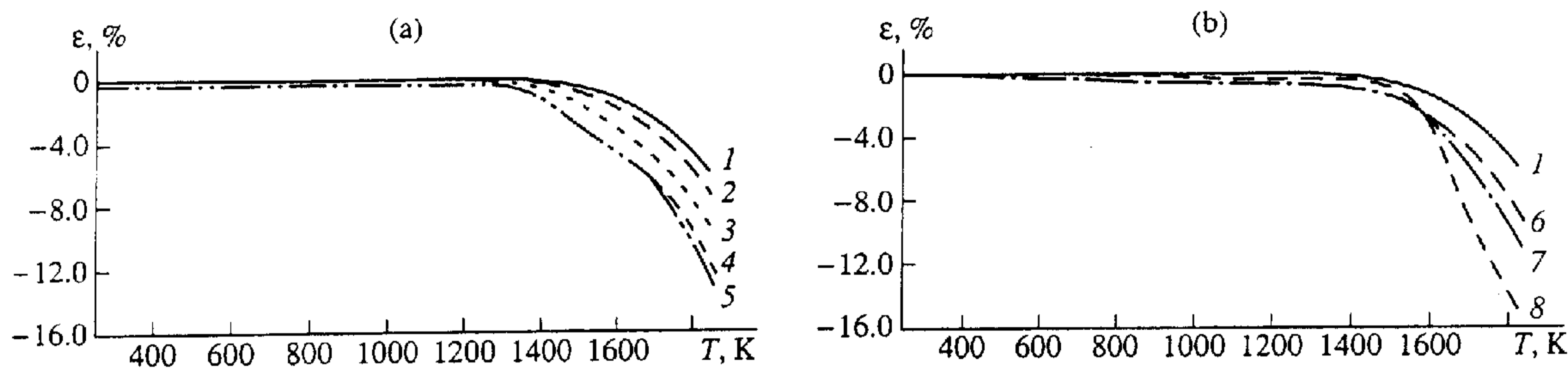


Fig. 3. Relative elongation during heat treatment of samples prepared by (a) molecular layering and (b) mechanical mixing. Curve numbers correspond to sample numbers in Table 3.

components in the $\text{AlO}_{1.5}\text{-TiO}_2$ and $\text{AlO}_{1.5}\text{-FeO}_{1.5}$ systems and considering the kinetics of the transition of the autonomous Fe(III) oxide phase to the nonautonomous phase conjugated with alumina grains, we infer that a similar transition in the $\text{AlO}_{1.5}\text{-TiO}_2$ system should have a relaxation time of the same order of magnitude (10^3 s).

Table 2. The difference between surface energies of components for several oxide systems

System	$\Delta\sigma, * \text{ J/m}^2$		
	1200 K	1400 K	1600 K
BeO- $\text{AlO}_{1.5}$	1.05	1.02	1.00
BeO- $\text{FeO}_{1.5}$	1.31	1.27	1.24
MgO- $\text{AlO}_{1.5}$	1.11	1.05	1.01
MgO- $\text{FeO}_{1.5}$	1.37	1.30	1.25
MgO- SiO_2	1.34	1.28	1.22
MgO- TiO_2	1.43	1.36	1.31
$\text{AlO}_{1.5}\text{-FeO}_{1.5}$	0.26	0.25	0.24
$\text{AlO}_{1.5}\text{-SiO}_2$	0.23	0.23	0.22
$\text{AlO}_{1.5}\text{-TiO}_2$	0.32	0.31	0.30
$\text{SiO}_2\text{-FeO}_{1.5}$	0.03	0.03	0.03

* $\Delta\sigma$ values calculated from the data of Bruce [18, 19].

Table 3. Density of alumina-based samples annealed at constant heating rates

Sample no.	TiO_2 weight fraction	Method of introducing TiO_2	$\rho, * \%$
1	0	—	58.1
2	0.0010	ML**: 1 cycle	57.3
3	0.0018	ML: 4 cycles	57.9
4	0.0022	ML: 6 cycles	56.8
5	0.0029	ML: 8 cycles	55.9
6	0.0010	MM***	58.8
7	0.0020	MM	57.6
8	0.0050	MM	59.4

*The relative density of unannealed compacted samples.

**Molecular layering.

*** Mechanical mixing.

Measurements showed (Fig. 3) that the samples prepared by mechanical mixing (Samples 6 - 8 in Table 3) start contracting about 10^3 s later than those prepared by molecular layering (Samples 2 - 5 in Table 3). This fact confirms the above conclusion that sintering is activated only after the 2D nonautonomous phase, conjugated with the bulk autonomous phase of the major component, is liquefied.

Simultaneously with the local equilibration at the boundaries of alumina grains, chemical potentials of the autonomous and nonautonomous phases become closer as a result of two processes. The first is a decrease in the Gibbs energy of the TiO_2 -based nonautonomous liquid phase A, and the second is a decrease in the Gibbs energy of the autonomous phase B. It is reasonable to consider these two processes separately because they differ in mechanisms and rates. The first process consists in the transition of the components of the autonomous phase contacting with the 2D nonautonomous phase to this latter phase. This process is fast because it does not involve large displacements of the particles, as the nonautonomous phase has a small dimension in the displacement direction [12]. This process is especially fast if the temperature exceeds $T_{m(2-n)}$, and the film of the molten TiO_2 -based nonautonomous phase is thinner than that existing at local equilibrium [12]. In this case, the process consists in the dissolution of the solid in the nonautonomous liquid phase. If the molten TiO_2 film has an equilibrium thickness, the transition of the components of the autonomous phase to the nonautonomous phase is accompanied by the transfer of Ti ions into the solid autonomous phase. In this case, the relaxation process will be substantially slower because of the low diffusion rates in alumina crystals, and the relaxation time will be comparable to that of process B, whose rate-limiting stage is impurity diffusion in the autonomous solid phase.

At $T \approx T_{m(2-n)}$, the equilibrium thickness of the layer of the TiO_2 -based 2D nonautonomous phase is ≈ 1 nm [12]. On the other hand, the maximum thickness of the TiO_2 layer deposited in one molecular-layering cycle is 0.23 nm. Therefore, to produce a locally equilibrated

layer of the 2D nonautonomous phase that does not need extra material translation, no less than five deposition cycles should be conducted.

If the 2D nonautonomous phase contains higher proportions of alumina, its equilibrium thickness is larger because its Gibbs energy is lowered due to a mixing-energy contribution [12]. At the same time, the viscosity of the liquid nonautonomous phase is then increased, which slows the sintering of alumina powder in comparison to a TiO_2 nonautonomous phase.

The suggested transformation and transport mechanisms involved in the sintering of TiO_2 -modified alumina are confirmed by the manner in which the linear dimensions of compacted samples of this material vary during heat treatment (Fig. 3).

CONCLUSION

The efficient method for introducing additives activating solid-state processes can be chosen based on the difference in surface energy $\Delta\sigma$ between the major and impurity phases. At $\Delta\sigma > 1 \text{ J/m}^2$, the additive effects on the solid-state processes are nearly independent of the manner in which the impurity was introduced. At $\Delta\sigma \leq 0.5 \text{ J/m}^2$, the most efficient methods are those that provide the best contact between components, molecular layering being an example. The amount of impurity that provides maximum activation effect is determined by the proportion of the locally equilibrated 2D nonautonomous phase in the temperature range of the process to be activated.

REFERENCES

1. Tammann, G., *Lehrbuch der Metallkunde: Chemie und Physik der Metallen und ihrer Legierungen*, Leipzig: Voss, 1932.
2. Tret'yakov, Yu.D., *Tverdogaznye Reaktsii (Solid-State Reactions)*, Moscow: Khimiya, 1978.
3. Gorshkov, V.S., Savel'yev, V.G., and Fedorov, N.F., *Fizicheskaya Khimiya Silikatov i Drugikh Tugoplavkikh Soedinenii (Physical Chemistry of Silicates and Other Refractory Compounds)*, Moscow: Vyssh. Shkola, 1988.
4. Andrievskii, R.A., *Sintering of Refractory Compounds, Aktual'nye Problemy Poroshkovo Metallurgii (Problems of Powder Metallurgy)*, Roman, O.V. and Arunachalama, V.S.M., Eds., Moscow: Metallurgiya, 1990.
5. Gusarov, V.V. and Suvorov, S.A., *Fazobrazovanie i Svoistva Materialov v Sistemakh BeO-AlO_{1.5}-MeO_n, Me = 3d-Element, Ga (Phase Formation and Material Properties in the BeO-AlO_{1.5}-MeO_n Systems, Me = 3d-Element or Ga)*, Available from ONITEKHIM, 1988, Cherkassy, no. 787-XII.
6. Gusarov, V.V. and Suvorov, S.A., *Melting Temperature of Locally Equilibrated Surface Phases in Polycrystalline Materials Based on a Single Bulk Phase*, *Zh. Prikl. Khim.* (Leningrad), 1990, vol. 63, no. 8, pp. 1689 - 1694.
7. Gusarov, V.V. and Suvorov, S.A., *Transformations of Nonautonomous Phases and Contraction of Polycrystalline Systems*, *Zh. Prikl. Khim.* (Leningrad), 1992, vol. 65, no. 7, pp. 1478 - 1488.
8. Defay, R. and Prigogine, I., *Tension Superficielle et Adsorption*, Liège: Éditions Desor, 1951.
9. Gusarov, V.V., *Thermodynamics of the Systems of Conjugated and Separated Regular Phases of Variable Composition, VI Vsesoyuzn. Simp. po Izomorfizmu (VI All-Union Symp. on Isomorphism)*, Moscow, 1988, p. 64.
10. Gusarov, V.V. and Suvorov, S.A., *Transformational and Transport Processes in Polycrystalline Systems in Relation to Material Creep*, *Zh. Prikl. Khim.* (Leningrad), 1992, vol. 65, no. 10, pp. 2377 - 2380.
11. Gusarov, V.V. and Suvorov, S.A., *High-Rate Thermally Induced Contraction of Materials*, *Zh. Prikl. Khim.* (Leningrad), 1993, vol. 66, no. 3, pp. 525 - 530.
12. Gusarov, V.V. and Suvorov, S.A., *The Thickness of 2D Nonautonomous Phases in Locally Equilibrated Polycrystalline Materials Based on a Single Bulk Phase*, *Zh. Prikl. Khim.* (Leningrad), 1993, vol. 66, no. 7, pp. 1529 - 1534.
13. Gusarov, V.V., Malkov, A.A., Malygin, A.A., and Suvorov, S.A., *The Powder Compounds with Nanostructures on the Surface (Synthesis, Properties, Applications)*, *II Int. Conf. on Nanometer Scale Science and Technol.*, Moscow, 1993, p. 10.
14. Gusarov, V.V., Malkov, A.A., Malygin, A.A., and Suvorov, S.A., *Formation of Aluminum Titanate in the Systems with High Spatial and Structural Conjugation of Components*, *Zh. Obshch. Khim.*, 1994, vol. 64, no. 5, pp. 971 - 977.
15. Gusarov, V.V., Egorov, F.K., Ekimov, S.P., and Suvorov, S.A., *Mössbauer Study on the Kinetics of Film Formation upon Interaction of Magnesium and Iron Oxides*, *Zh. Fiz. Khim.*, 1987, vol. 61, no. 6, pp. 1652 - 1654.
16. Semin, E.G., Lukin, Yu.N., and Andreeva, N.A., *The Dynamics of BeO Contraction and Grain Growth in the Presence of Iron Oxide*, *Izv. Akad. Nauk SSSR, Neorg. Mater.*, 1986, vol. 22, no. 4, pp. 623 - 627.
17. Semin, E.G., Golovlev, G.A., Gusarov, V.V., et al., *Kinetics of BeO Contraction and Grain Growth in the Presence of Aluminum Oxide*, *Neorg. Mater.*, 1992, vol. 28, no. 4, pp. 793 - 799.
18. Bruce, R., *Calculating Free Surface Energy for Ceramics Materials*, *Science of Ceramics: Proc. Conf. of the British Ceramic Society and Nederlandse Keramische Vereniging*, Stewart, G.H., Ed., London: Academic, 1962.
19. Bruce, R., *Calculating Average Free Surface Energy and the Contribution of Certain Variables*, *Science of Ceramics: Proc. Conf. of the British Ceramic Society and Nederlandse Keramische Vereniging*, Stewart, G.H., Ed., London: Academic, 1962.
20. Aleskovskii, V.B., *Stekhiometriya i Sintez Tverdykh Soedinenii (Stoichiometry and Synthesis of Solids)*, Leningrad: Nauka, 1976.
21. Kol'tsov, S.I., *Principles and Problems of Chemical Design of Solids*, *Aktual'nye Problemy Khimii Tverdykh Veshchestv: Mezhevuzovskii Sbornik Nauchnykh Trudov (Problems of Solid State Chemistry: Collected Works of High-School Institutions)*, Leningrad: LTI, 1992, pp. 7 - 15.